Senior Thesis

Volcanoes as Indicators of Regional Stress Orientation in the Erebus Volcanic Province, West Antarctica

by
Adam Angel
1995

Submitted as partial fulfillment of
the requirements for the degree of
Bachelor of Science in Geology and
Mineralogy at The Ohio State University,
Spring Quarter, 1995

Approved by:

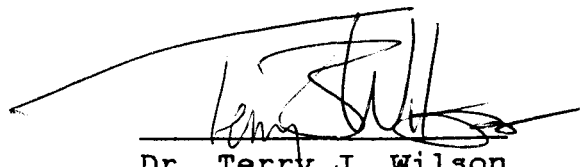

Dr. Terry J. Wilson

Table of Contents

INTRODUCTION

The international World Stress Map project shows that there are almost no stress data from the Antarctic plate (Fig. 1). In other continents stress information is available from various types of geophysical and geological data, including earthquake focal mechanisms, well bore breakouts, in situ measurements (hydraulic fracturing, overcoring), and from young faults and volcanic alignments (Table 1). In Antarctica, remoteness, aseismicity, ice cover, and a lack of commercial drilling have precluded geophysical and in situ measurements. Antarctica does however have an abundance of Cenozoic volcanic activity and young faulting associated with the West Antarctic Rift system (Fig. 2). Therefore, the purpose of this study is to use volcanic cone patterns in part of the Erebus Volcanic Province (EVP), near the western margin of the West Antarctic rift system, to evaluate a contemporary stress pattern in this section of Antarctica. If the present-day lithospheric stress field is studied, then plate driving forces will better be understood. The new stress data will also provide information on the neotectonic evolution of the Antarctic lithosphere including

- reasons for aseismicity.
- a stress configuration for Transantarctic Mountain uplift and West Antarctic rifting.
- regional neotectonic environment in relation to global

tectonics.

- an Antarctic intraplate stress field.

The study of the proposed area in the EVP will show the orientation of the average tectonic stress during the evolution of certain polygenetic volcanoes. This is possible because non-magmatic stresses must also be reflected in volcanic flank eruption trends, which approximate radial dike patterns (Nakamura, 1977).

STRESS DETERMINATIONS FROM VOLCANIC ALIGNMENTS

According to Nakamura (1977), volcanic vent alignments formed above subsurface feeder fissures and intrusive dikes represent natural hydrofractures formed due to magma pressure. The dikes, commonly vertical, and the alignments should form perpendicular to S_{hmin}, and parallel to S_{hmax}. In areas of Quaternary volcanism, the underlying feeder dike system is not likely to be exposed yet. Therefore, it becomes necessary to infer alignments from linear zones of cinder cones or other vents to determine contemporary stress.

FLANK ERUPTIONS ON POLYGENETIC VOLCANOES

Magmatic pressure in a volcanic conduit increases to the sum of the tensile strength of surrounding rocks and the minimum

compressional stress of external origin. If pressure is not adequately relieved by a summit eruption, then a vertical fracture develops laterally, causing a flank or flank-fissure eruption (Fig. 3) (Nakamura, 1977).

Radial dikes show that magmatic pressure in the central conduit of a composite volcano was predominant over external forces or that external horizontal forces were equal (Fig.4A). However, radial dikes can curve at a sufficient distance from the central conduit and assume one general trend paralleling the greatest compressional force (Fig.4B). An elongated central plutonic complex is another signature of the influence of imposed horizontal stresses.(Nakamura, 1977).

In a situation where a volcano lies on a tilted surface, a differential stress in the horizontal plane can be produced by gravitational force. When a shield volcano grows on the slope of an adjacent volcano, gravity produces a tensional stress in the overlying volcanic structure. This tensional stress is in the direction of the basal surface inclination, and may control radial dike trends. If gravitational force is the dominant control on dike trends, then the trend of the whole zone of flank eruptions can be curved to follow the underlying relief. Where flank eruptions form linear trends, but there is no consistent orientation between neighboring volcanoes, this may indicate a dominant gravitational influence. Alternately, where flank eruptions create a linear zone intersecting the summit and form a continuous linear or curvilinear trend amongst adjacent

volcanoes, then the fundamental stress governing the trend can be ascribed to a regional tectonic stress (Nakamura, 1977).

Accepting the surface of the Earth is a free surface and a general triaxial compressive stress field, one principal stress will be vertical and the other two horizontal. Dikes should thus form vertical trends perpendicular to the minimum horizontal stress, or least principal stress. The trend of the linear dike array could be parallel to either the maximum or intermediate principal stress, corresponding to a regional contractional or extensional tectonic regime respectively. If the sense of displacement of active faults in the same area is known, a distinction can be made between contractional and extensional tectonic stress fields. Strike-slip and/or thrust faults accompany an area with a contractional tectonic regime, and have flank crater zones oblique to the fault trends. Flank crater trends are approximately 45 degrees to strike-slip faults and are perpendicular to the thrust faults (Fig. 5) (Nakamura, 1977).

If faults are absent for distinguishing between extensional and contractional regimes, then the angular relationship between the trend of the volcanic belt and zones of flank craters will distinguish between the two (Fig.5). Figure 5B shows that in a contractional tectonic area, with maximum compressional stress horizontal, the two trends form a high angle with each other. Fig. 5A shows that in an extensional tectonic area, with maximum compressional stress vertical, the two trends are approximately parallel. This angular relationship corresponds with volcanic

belts under contractional and extensional tectonics, respectively. Extensional volcanic belts and accompanying zones of flank eruptions tend to be perpendicular to the divergence direction between plates. Contractional tectonic area volcanic belts parallel the convergence direction across the plate boundary. The maximum compressional stress in the volcanic belt will be nearly parallel to the converging direction and form an angle between the zone of flank eruptions and the trend of the volcanic belt (Nakamura, 1977).

VENT ALIGNMENTS IN VOLCANIC FIELDS

Multiple eruptions in a given area will form a field of scattered vents and cinder cones. Due to the linear character of magmatic hydrofractures, any one given eruption can produce multiple vents, and it is difficult to determine these vent alignments from visible cinder cones (Fig. 6). The goal is to statistically produce and reproduce these vent alignments (Fig. 7) (Wadge and Cross, 1988).

One way to define volcanic alignments is by midpoint, strike, and length. Alignments are chosen by inspection and the strike is then determined by a linear least squares fit. The standard deviation of the fit is used to determine the quality of the proposed alignment along with the number of vents. The quality rating is grouped into four ranks, A >B >C >D, where A ≥5 vents, and B = 4 vents. When the standard deviation of the fit

SD ≤750m, no penalty is applied to the alignment. A penalty of one rank is applied where 750m < SD < 2250m, and a penalty of three ranks applied where SD > 2250m (Suter et al., 1992).

There are two other quantitative methods for determining the directions of lineaments defined by aligned volcanic vents. The two-point azimuth and Hough transform methods are two effective procedures, which can compliment each other and generate reproducible results.

The two-point azimuth method checks the whole field of mapped vent sites and tests whether alignments are significant or due to chance. First, every azimuth between a given point and all other points is measured. For a total of n points there will be $n(n-1)/2$ azimuths that may or may not show a preferred direction. The problem is that an elongated field of study will produce more azimuths with that orientation. This problem can be fixed by using a circular field or by correcting for the shape of the field. By using a set of circular fields (bins), a correction for field elongation can be made. Each bin is treated separately and given a correction based on $C=of(exf/sf)$, where C is the correction, of is the observed frequency, exf is the expected mean frequency, and sf is the simulated frequency. The result can be displayed as a histogram of azimuth frequency for each bin. Ideally, this method should be used in a field of homogeneously distributed points. Therefore, in a heterogenous field, the same number of points is used in each bin (Wadge and Cross, 1988).

The Hough transform method plots given points from a geometric feature onto a plane. Three collinear points can be defined by the length of the normal (φ) to the origin, and the angle (θ) between that normal and the x-axis (Fig. 8A). The equation of the line ($\varphi = x\cos\theta + y\sin\theta$) can now be used as the axes of a new parameter plane that corresponds to φ and θ (Fig. 8B). φ is calculated for successive values of θ with respects to all (x,y) values and creates a sinusoidal curve in the parameter plane. Therefore, each point on the curve represents a line which contains a fixed point (x,y), and each curve will intersect at a common point. This common point represents the accepted alignment (Wadge and Cross, 1988).

Histograms serve to display the results of the two-point azimuth method. Observed, simulated, shape-corrected, region-corrected, and circular sample plots will show frequency of azimuthal direction based on 180 degrees. This analysis is effective on a regional scale. The results of the Hough transform method will also be displayed as a histogram. First, the parameters must be set for window diameter (w), quantization intervals for $\Delta\varphi$ and $\Delta\theta$, minimum number of collinear vents (T), and rank order of lines (R). The histogram, in this method, serves only as an indicator of frequency at one set of given parameters. Therefore, this analysis is effective on a local scale. Zoback (1992) created a quality ranking scheme with five ranks, A > B > C > D > E (Table 1). A rank of A is assigned to an alignment where five or more vent alignments, or parallel

dikes, are present with a standard deviation of less than 12 degrees. A rank of B is assigned to an alignment where three or more vent alignments, or parallel dikes, are present with a standard deviation of less than 20 degrees. A rank of C is assigned to an alignment where there is a single well exposed dike or a single alignment. A, B, and C vent alignments must consist of at least five vents. A rank of D is assigned when an alignment has be inferred from less than five vents. A rank of E is assigned when no reliable information is available regarding principal stress orientations. Lastly, rank A is considered to be accurate within ±10-15 degrees, rank B within ±15-20 degrees, rank C within ±25 degrees, and D yielding questionable results.

POTENTIAL AMBIGUITIES AND PROBLEMS

The primary problem with vent alignment analysis is that pre-existing joint sets, when close to the surface, may control intrusion rather than magma inducing fractures as required to apply stress analysis. However, the errors created by preexisting fault sets will be small. For a previously existing joint set to be intruded into, its strike must be nearly perpendicular to the greatest tensional stress. The error can be great when the two horizontal stresses are approximately equal, but this scenario rarely occurs (Zoback, 1992). The Chyulu Hills in Southeastern Kenya and the Springerville Volcanic Field in Arizona exhibit this problem and provide insight on tectonic

stress regimes of the past, as well as exposing the ambiguities inherent in using this method.

EXAMPLES CARRIED OUT WITH PROPOSED METHODS

An area in the East African Rift System that can be used to determine a stress field history is the Chyulu Hills on the eastern shoulder of the Kenya Rift. This area is characterized by a NW-SE orientation of regional extensional stress (Bosworth et al., 1992). This orientation has rotated from a Pleistocene E-W orientation. The Huri Hills, Marsabit, and Nyambeni volcanic fields all have a minimum compressional stress orientation of 135 degrees (Fig. 9). The Chyulu Hills, however, exhibit a different alignment and may belong to a separate stress-field province. Another possibility is that this volcanic field orientation belongs to the same stress field province and has simply been controlled by regional joint set patterns (Haug and Strecker, 1995).

Figure 10 shows vent alignments and normal faults in the northern Chyulu Hills. Group 1 Quaternary volcanic rocks (~1.4 Ma) through Group 5 Quaternary volcanic rocks (youngest) decrease in weight percent SiO_2 with age (Fig. 11). Groups 1-4 volcanic chains trend NW-SE in basement rock joints, and parallel NW-SE striking normal faults. Group 5 volcanoes, the only group to exhibit a NNE alignment, have younger NNE faults cutting the older NW-SE striking volcanics and normal faults. In figure 10,

steep east dipping normal faults between Simba and Kiboko offset Holocene alluvium on the order of 2 to 10 m (Haug and Strecker, 1995).

The pre-existing NW-SE trending joint sets are in amphibolite-grade gneisses and are commonly occupied by quartz-feldspar pegmatites. The vents belonging to groups 1-4 in the Chyulu Hills parallel these joints. Since the pre-existing joints formed in the Late Proterozoic, it can be assumed that they have no relation to the Late Cenozoic stress field. Therefore, the joints merely guided the ascent of magmas during the past 1.4 Ma (Haug and Strecker, 1995).

This problem occurs because a small range of joint orientations can be intruded if they form a high enough angle with the least compressional stress orientation. (This varies with the magnitude of magma pressure.) Since study of the Kenya rift shows an approximate E-W orientation of least compressional stress in Neogene and Mid-Pleistocene times, the basement anisotropies in the Chyulu Hills apparently formed a high angle with this stress. Therefore, assuming sufficient magma pressure, groups 1-4 do not directly reflect the orientation of stress. Group 5, however, does reflect the regional stress orientation, which is exhibited in the cross-cutting relationships of the more recent faulting with the older faulting. The existing anisotropies are no longer intruded, because the current stress orientation forms a very low angle with them. Lastly, as this angle became lower and lower, the pressure on the country rock

increased (prior to new faulting) and caused the intrusions to become more felsic (Haug and Strecker, 1995).

The Springerville Volcanic Field (SVF), Arizona is an example where cluster analysis, the Hough transform, and the two-point azimuthal methods have been used to compare cinder cone distribution with regional crustal structure. Together, this information has implications for the stress field around the SVF. Most volcanism on the southern part of the Colorado Plateau (CP) has been concentrated in seven volcanic fields along the margins of the plateau. SVF, the southernmost of the seven fields, straddles the Mogollon Rim forming the physiographic boundary between the CP and the Transition Zone (TZ) (Fig. 12) (Connor et al., 1992).

The SVF consists of 409 vents covering approximately 3000 km^2. It is just north of Mount Baldy, a 7-9 ma trachyte shield volcano. The vents are mainly cinder cones with some spatter cones, two shield-type volcanoes, four fissure vents, and five maar craters. The vents used in this particular study were active between 2.1 and .3 ma (decreasing from west to east) and produced approximately 300 km^3 of 47 vol % alkali-olivine basalt, 28 vol % hawaiite, 24 vol % tholeiite, and 1 vol % mugearite and benmoreite.

Out of 409 vents, 404 were used to distinguish seven clusters of different ages. Age variation was marked in relation to petrologic differences. The prominent alignments are WNW in the western SVF and ENE in the eastern SVF. The point at which

these two trends meet in the south central SVF marks the most intense cinder cone density. Cluster distribution and age variation would seem to indicate that these vent alignments are due to magma ascension along preexisting faults and fractures. These extensional features are most likely related to regional physiographic features such as the Colorado Plateau (Connor et al., 1992).

TECTONIC SETTING AND GEOLOGY OF THE EREBUS VOLCANIC PROVINCE

NEOTECTONIC SETTING OF ANTARCTICA

The Antarctic plate is encircled by mid-ocean ridges and transform faults excepting the boundary between South America and the tip if the Antarctic Peninsula (Fig. 13). Continually moving plate boundaries have not perceptibly moved the plate in Neogene time, or even perhaps in 80 Ma. Plate immobility is supported by the lack of linear hotspots in continental and oceanic volcanoes on the Antarctic plate. The Hallett province and Marie Byrd Land (MBL) contain linear volcanoes, but with no evidence of migration of activity or relation to plate motions (LeMasurier, 1990).

Vertical displacement and extension, related to intracontinental rifting, characterize the Cenozoic tectonic regime, although the plate margins would be expected to create a compressional intraplate stress field (LeMasurier, 1990). At the present time earthquakes are not occurring in Antarctica. This

could reflect modern tectonic quiescence that might follow a period of high post-deglaciation seismicity. However, seismicity might also be suppressed by the combination of vertical loading by the Antarctic Ice Sheet and a compressional intraplate stress field. In addition to little seismic activity, borehole stress measurements are not available on the Antarctic continent due to remoteness, ice cover, and lack of commercial drilling.

Subduction-related volcanoes in Graham Land (GL) and the South Shetland Islands (SSI) are remnants of a Cretaceous active plate margin that stretched along the entire Pacific margin of the combined Antarctic-New Zealand (NZ)-Campbell Plateau (CP) continent. Around 80 Ma the NZ-CP block rifted from MBL and created the present rifted continental margin. Subduction terminated systematically northeastward until 4 Ma when it stopped at the tip of the Antarctic Peninsula. Therefore the northern Antarctic Peninsula consists of arc, back-arc, and within plate environments that overlap within 10 Ma (LeMasurier, 1990).

The West Antarctic rift system is a zone of lithospheric weakness that has shown extensive volcanism and extensional strain. Jurassic rifting parallels the line of the Late Cretaceous breakaway of the NZ-CP block. The rift zone also parallels the boundaries of the Late Mesozoic and Early Paleozoic active plate margins (fig. 14). The regional extent of the West Antarctic Rift is difficult to define due to the deceptive arrangement of Cenozoic volcanic fields, which suggest a primary

relationship to the continental margin. While there is no continuous sub-sea level topographic low along the Transantarctic Mountains (TAM), there is a pronounced trough between the Ross and Bellingshausen Seas. Here the maximum depth reaches -2555 m in the Bentley Subglacial Trench and -2000 m in the Byrd Subglacial Basin (Fig. 15). Pre-Cenozoic basement rock along the TAM is over 4000 m in elevation in many peaks, and descends across the front to between -2500 m and -4500 m at the rift axis. In the horsts and grabens of MBL the basement rock varies between -3000 m and +2700 m (Fig. 15). Much of the subglacial topography could be a product of late Cenozoic tectonic displacement, if glacial ice behaves as basin fill in the trough, and the ages of flanking volcanic fields and vertical fault displacement of the early Tertiary erosion surface in MBL are indicative (LeMasurier, 1990).

Seismic data shows crustal thicknesses to range from a minimum of 25 km along the length of the Ross-Bellingshausen topographic trough to 32 km in Marie Byrd Land, 36 km in the Ellsworth Mountains, and 40 km in East Antarctica (Bentley, 1973). The trough is characterized by a broad negative isostatic gravity anomaly (-10 to -20 mGals), with four narrow positive anomalies (+10 to 30 mGals) flanking on both sides (Bentley, 1982). The broadness of the negative trough anomaly can be interpreted as the gravity signature of sedimentary rock. These geophysical characteristics are similar to those of the East African rift, the Rio Grande rift, and the Oslo graben

(LeMasurier, 1990).

Cenozoic volcanoes are arrayed along the flanks of the West Antarctic rift from the western Ross Embayment to Palmer Land . Volcanoes from the Adare Peninsula to Mount Early lie on the east Antarctic flank, Marie Byrd Land volcanoes lie on the Pacific flank, and volcanoes lie on both flanks in Ellsworth Land, Palmer Land, and Alexander Island. The volcanically and structurally asymmetrical rift has the largest volumes of basaltic and felsic rock, as well as the longest duration of activity, in the western Ross Embayment and Marie Byrd Land provinces. These provinces were active in the early Miocene, late Oligocene, and possibly in the Late Eocene. Volcanic centers are small, scattered, basaltic and Late Miocene to Recent around the Bellingshausen Sea at the eastern end of the rift (LeMasurier, 1990).

CENOZOIC MCMURDO VOLCANIC GROUP

The McMurdo Volcanic Group (MVG) refers to all Cenozoic volcanic rocks in and next to the TAM and the western Ross Embayment (Ross Sea and Ross Ice Shelf) (Fig. 16). This group is comparable in size with the East African Rift system and forms one of the most extensive alkali volcanic provinces in the world (Kyle, 1990a). The group is divided into the Hallett, Melbourne and Erebus volcanic provinces based on spatial and tectonic characteristics. Volcanic centers in the MVG range from >1800 km^3 (Mt. Erebus) to small scoria cones. Mt. Erebus is the

southernmost active volcano on Earth. It has a permanent convecting anorthoclase phonolite lava lake in a 3794 m high summit crater. Small Strombolian type eruptions occur several times a day (Kyle, 1990a).

The MVG distribution is controlled by two tectonic elements: 1) The TAM are a major uplifted, block-faulted range extending over 3000 km across Antarctica. 2) The Ross Embayment and a major normal fault zone between it and the TAM. Crustal thickness changes from 40 km beneath the TAM to 25 km beneath McMurdo Sound and Ross Island across this fault boundary (Kyle, 1990a).

The Victoria Land basin (VLB) is the westernmost basin in the Ross Sea. There is over 12 km of sediment in the Victoria Land basin which extends from Ross island to Cape Washington. The basin contains the Discovery graben and the Lee arch that comprise the Terror Rift. The Terror rift is marked in the north by Mount Melbourne and in the south by Mount Erebus, both of which are currently active (Kyle, 1990a).

EREBUS VOLCANIC PROVINCE

The Erebus volcanic province (EVP), at the southern end of Terror rift (Fig. 16), occurs at a TAM trend change and where several TAM bounding faults might intersect. Trachytic rocks were dominant from about 19 Ma to about 10Ma, and increased activity in the last 10 m.y. is mainly basanitic and phonolitic

(Kyle, 1990a). Figure 17 shows generalized ages in the EVP based primarily on K-Ar age determinations. Each volcanic center appears to have been active for ~ 1-2 m.y., with the oldest center being around the base of Mount Morning. The oldest centers are Gandalf and Riviera Ridges, and Mason Spur at 18.7-12.4 Ma. A migration to the northeast is evidenced by the age determinations for eastern Minna Bluff (11-9 Ma), northern Black Island (10.9 Ma), central Minna Bluff (8.3-7.3 Ma) and Mount Discovery (5.3-4.4 Ma). 4 Ma marks an increase in volcanic activity with the formation of Mount Bird (4-3 Ma), Mount Terror (2-0.6 Ma), Hut Point Peninsula (1.8-0.4 Ma), and Mount Erebus (<1 Ma) (Kyle, 1990b).

PREVIOUS STRUCTURAL MODELS FOR THE EREBUS VOLCANIC PROVINCE

Kyle and Cole [1974] thought that Mt. Bird, Mt. Terror, and the Hut Point Peninsula displayed a radial pattern around Mt. Erebus at 120 degree angles (Fig. 18). This would fit a model for radial fractures formed in a crustal doming process. *Kyle et al.* [1989] proposed that in order to supply Mt. Erebus with the volume of phonolite erupted, it needed a mantle plume or hot spot beneath it. The doming that created the radial symmetry displayed on Ross Island could be due to the initiation of that mantle plume (Kyle, 1990b).

According to Kyle and Cole (1974), Mt. Discovery also displays a radial symmetry, and could be an early expression of

the Mt. Erebus mantle plume. The flanking vents of Minna Bluff, Brown Peninsula, and Mt. Morning are at 120 degree angles to each other with respect to Mt. Discovery (Kyle, 1990b).

Wright-Grassham (1987) thought that a lineament defined by Mt. Morning, Mt. Discovery, Black Island, and White Island was indicative of a transfer fault terminating the Terror rift (Fig. 19). The Discovery Volcanic Subprovince (DVS) has had continuous volcanic activity over the last 19 Ma and is therefore the most complete record of eruptive and tectonic styles in the MVG (Wright-Grassham, 1987).

Figure 19 shows four structural trends that have been active at different times. The structural trends are NNW to N-S, NW, NE, and NNE. The NNW to N-S trends, which are not a major control of volcanic activity, can be observed at Gandalf Ridge as hydrothermal and alteration zones, dikes, and inferred vent alignments (Muncy, 1979). This feature could be reflective of axial faulting associated with the VLB and the eastern margin of the TAM. The NW trends are dike and vent alignments along Minna Bluff and dikes along Mason Spur. (Black Island exhibits this trend in its oldest deposits, but to a much lesser extent.) This trend may be controlled by upper crustal weaknesses, and would therefore be associated with NW-trending F_2 fold axes. The NE trend is an inferred alignment of young phonolite stratovolcanoes on Mt. Morning, Mt. Discovery and Mt. Aurora. If these three stratovolcanoes are aligned along a transform fault, which dextrally offsets the the TAM axial trend, then this area may

mark the southern limit of the VLB. The NNE trends are inferred from vents on Mt. Morning, Mt. Discovery, and Brown Peninsula, and indicate a NNE-trending fracture system that has been active for 5 Ma (Wright-Grassham, 1987).

Wright-Grassham (1987) thinks that the radial symmetry proposed by Kyle and Cole (1974) is not substantiated by current evidence. With Minna Bluff activity occurring ~ 8.3-7.3 Ma, Brown Peninsula activity occurring ~ 2.7-2.1 Ma, Mt. Morning activity occurring ~ 2.5-1 Ma, and Mt. Discovery activity occurring ~ 5.1-6.6 Ma, it seems that any crustal doming occurred too late to influence Minna Bluff volcanism.

DISCUSSION

A preliminary attempt to map the position of volcanic cones in the Mt. Discovery region of the EVP was made. This mapping was done using a Landsat-4 Thematic Mapper satellite image. Band 5 (a near-infrared wavelength band), which produces maximum geologic detail and limits saturation problems (extreme brightness) caused by ice-cover, was chosen for the Mt. Discovery region. To sharpen linear and curvilinear features, as well as the shapes of individual cones, the Band 5 image was filtered with a nondirectional high-pass filter. To enhance the volcanic features, the range of grey tones was extended by applying a contrast stretch to the image. The image processing was carried out by T. Wilson using the software package *ERDAS Imagine* at the

OSU Center for Mapping. When the image was enlarged to the limit of resolution (1 pixel = ground cell of 30 m), and examined together with aerial photography (to clarify ambiguities), it provides an accurate spatial representation of the cone distribution although not all of the cones could be resolved at this scale.

Mapping and analysis of the spatial distribution of the volcanic cones was not completed. However, this study showed that by looking at the vent alignments associated with Mt. Discovery, including the areas of Mt. Morning, Brown Peninsula, and Black Island, it would be possible to reconstruct the orientation of the average tectonic stress during the Cenozoic evolution of the region. Using either the two-point azimuthal method, the Hough transform method, or simple linear regression, the resultant orientation would be reproducible and have a higher confidence level than previous efforts determined by inspection. This information, when coupled with previously collected age and petrologic data, could provide critical information for the development of structural models in the EVP.

REFERENCES CITED

BOSWORTH,W., STRECKER,M.R., and BLISNIUK,P.M., 1992, Integration of East African paleostress and present-day stress data: implications for continental stress field dynamics. Journal of Geophysical Research, v. 97, no. B8, p. 11,851-11,865.

CONNOR,C.B., CONDIT,C.D., CRUMPLER,L.S., and AUBELE,J.C., 1992, Evidence of regional structural controls on vent distribution: Springerville volcanic field, Arizona. American Geophysical Union, p. 12,349-12,359.

HAUG,G.H., STRECKER,M.R., 1995, Volcano-tectonic evolution of the Chyulu Hills and implications for the regional stress field in Kenya. Geology, v. 23, no. 2, p. 165-168.

KYLE,P.R., and COLE,J.W., 1974, Structural control of volcanism in the McMurdo Volcanic Group, Antarctica. *Bull. of Volcanol.*, 38, 16-25.

KYLE,P.R., MOORE,J.A., and THIRLWALL,M.F., 1989, Petrologic evolution of anorthoclase phonolite lavas at Mount Erebus, Ross Island, Antarctica, *Journal of Petrology.*

KYLE,P.R., 1990a, Volcanoes of the Antarctic plate and southern oceans. *McMurdo Volcanic Group Western Ross Embayment.* Antarctic Research Series, 48.

KYLE,P.R., 1990, Volcanoes of the Antarctic plate and southern oceans. *Erebus Volcanic Province.* Antarctic Research Series, 48.

LEMASURIER,W.E., and THOMSON,J.W., 1990, Volcanoes of the Antarctic plate and southern oceans. Antarctic Research Series, 48.

NAKAMURA,K. 1977, Volcanoes as possible indicators of tectonic stress orientation - principle and proposal. Journal of Volcanology and Geothermal Research 2. 1-16.

SUTER,M., QUINTERO,O., and JOHNSON,C.A., 1992, Active faults and state of stress in the central part of the Trans-Mexican volcanic belt, Mexico 1. The Venta de Bravo Fault. Journal of Geophysical Research, vol. 97, no. B8, 11,983-11,993.

WADGE,G., CROSS,A., 1988, Quantitative methods for detecting aligned points: an application to the volcanic vents of the

Mochoacán-Guanajuato volcanic field, Mexico. Geology, 16, 815-818.

WRIGHT-GRASSHAM, 1987, Volcanic geology, mineralogy, and petrogenesis of the Discovery Volcanic Province, Southern Victoria Land, Antarctica. PhD. Thesis, New Mexico Institute of Mining and Technology, Socorro, New Mexico. 2V. 460

ZOBACK,M.L., 1992, First- and second-order patterns of stress in the lithosphere: The world stress map project. Journal of Geophysical Research, v. 97, no. B8, p. 11,703-11,728.

TABLE 1. Quality Ranking System for Stress Orientations (Zoback, 1992)

A	B	C	D	E
		Focal Mechanism (FM)		
Average P axis or formal inversion of four or more single-event solutions in close geographic proximity (at least one event $M \geq 4.0$, other events $M \geq 3.0$)	Well-constrained single-event solution ($M \geq 4.5$) or average of two well-constrained single-event solutions ($M \geq 3.5$) determined from first motions and other methods (e.g., moment tensor waveform modeling or inversion)	Single-event solution (constrained by first motions only, often based on author's quality assignment) ($M \geq 2.5$) Average of several well-constrained composites ($M > 2.0$)	Single composite solution Poorly constrained single-event solution Single-event solution for $M < 2.5$ event	Large historic event with no reliable focal mechanism Event with P, T, B axes all plunging 25°–40° Event with P and T axes both plunging 40°–50°
		Well Bore Breakout (IS-BO)		
Ten or more distinct breakout zones in a single well with s.d. ≤12° and/or combined length >300 m Average of breakouts in two or more wells in close geographic proximity with combined length >300 m and s.d. ≤12°	At least six distinct breakout zones in a single well with s.d. ≤20° and/or combined length >100 m	At least four distinct breakouts with s.d. <25° and/or combined length >30 m	Less than four consistently oriented breakouts or <30 m combined length in a single well Breakouts in a single well with s.d. ≥25°	Wells in which no reliable breakouts detected Extreme scatter of orientations, no significant mean determined (s.d. >40°)
		Hydraulic Fracture (IS-HF)		
Four or more hydrofrac orientations in single well with s.d. ≤12°, depth >300 m Average of hydrofrac orientations for two or more wells in close geographic proximity, s.d. ≤12°	Three or more hydrofrac orientations in a single well with s.d. <20° Hydrofrac orientations in a single well with 12° < s.d. ≤25°	Hydrofrac orientations in a single well with 20° < s.d. <25°; distinct hydrofrac orientaiton change with depth, deepest measurements assumed valid One or two hydrofrac orientations in a single well	Single hydrofrac measurement at <100 m depth	Wells in which only stress magnitudes measured, no information on orientations
		Petal Centerline Fracture (IS-PO)		
		Mean orientation of fractures in a single well with s.d. <20°		
		Overcore (IS-OC)		
Average of consistent (s.d. ≤12°) measurements in two or more boreholes extending more than two excavation radii from the excavation wall and far from any known local disturbances, depth >300 m	Multiple consistent (s.d. <20°) measurements in one or more boreholes extending more than two excavation radii from excavation well, depth >100 m	Average of multiple measurements made near surface (depth >5–10 m) at two or more localities in close proximity with s.d. ≤25° Multiple measurements at depth >100 m with 20° < s.d. <25°	All near-surface measurements with s.d. >15°, depth <5 m All single measurements at depth Multiple measurements at depth with s.d. >25°	Multiple measurements at a single site or locality with no significant mean (s.d. >40°)
		Fault Slip (G-FS)		
Inversion of fault-slip data for best fitting mean deviatoric stress tensor using Quaternary age faults	Slip direction on fault plane, based on mean fault attitude and multiple observations of the slip vector; inferred maximum stress at 30° to fault	Attitude of fault and primary sense of slip known, no actual slip vector	Offset core holes Quarry popups Postglacial surface fault offsets	Not complied
		Volcanic Vent Alignment (G-Va)*		
Five or more Quaternary vent alignments or "parallel" dikes with s.d. <12°	Three or more Quaternary vent alignments or "parallel" dikes with s.d. <20°	Single well-exposed Quaternary dike Single alignment with at least five vents	Volcanic alignment inferred from less than five vents	Not compiled

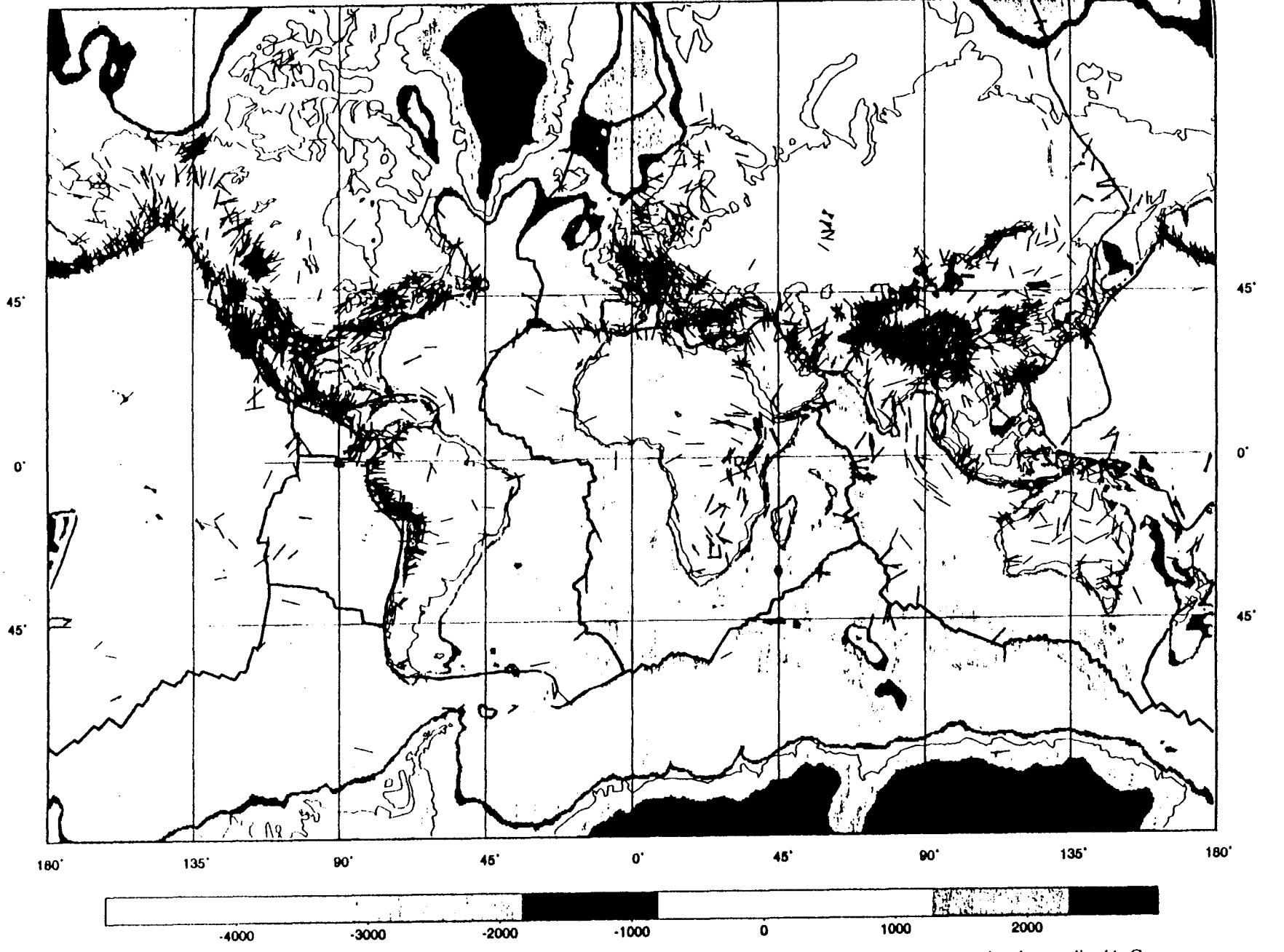

Fig. 1. World stress map: S_{Hmax} orientations plotted on a base of average topography. Line lengths of data proportional to quality (A–C data plotted, see Table 2). See Plate 1 for more detail, including type of indicator and stress regime for individual points.

(Zoback, 1992)

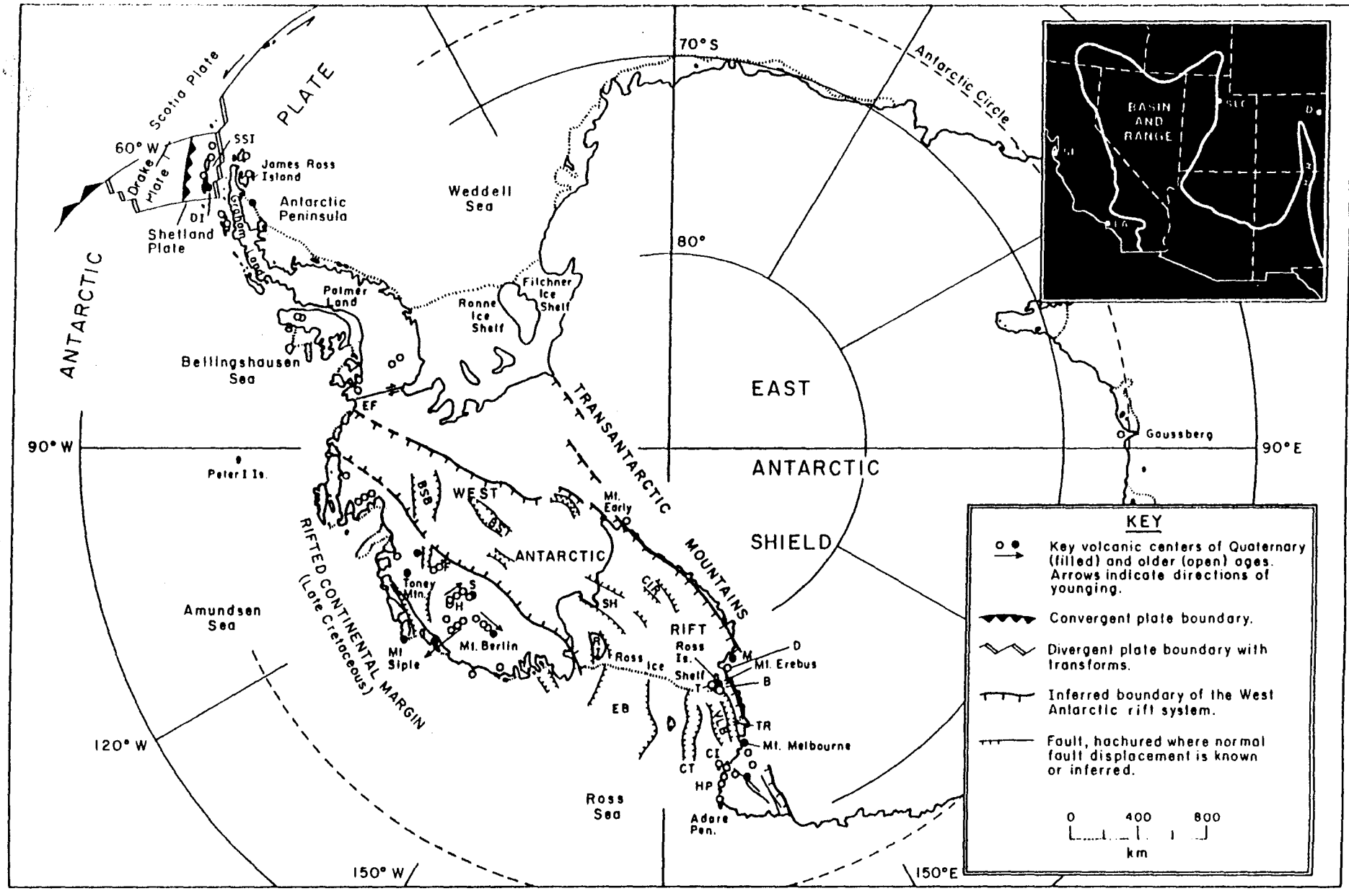

Figure 2 (LeMasurier, 1990)

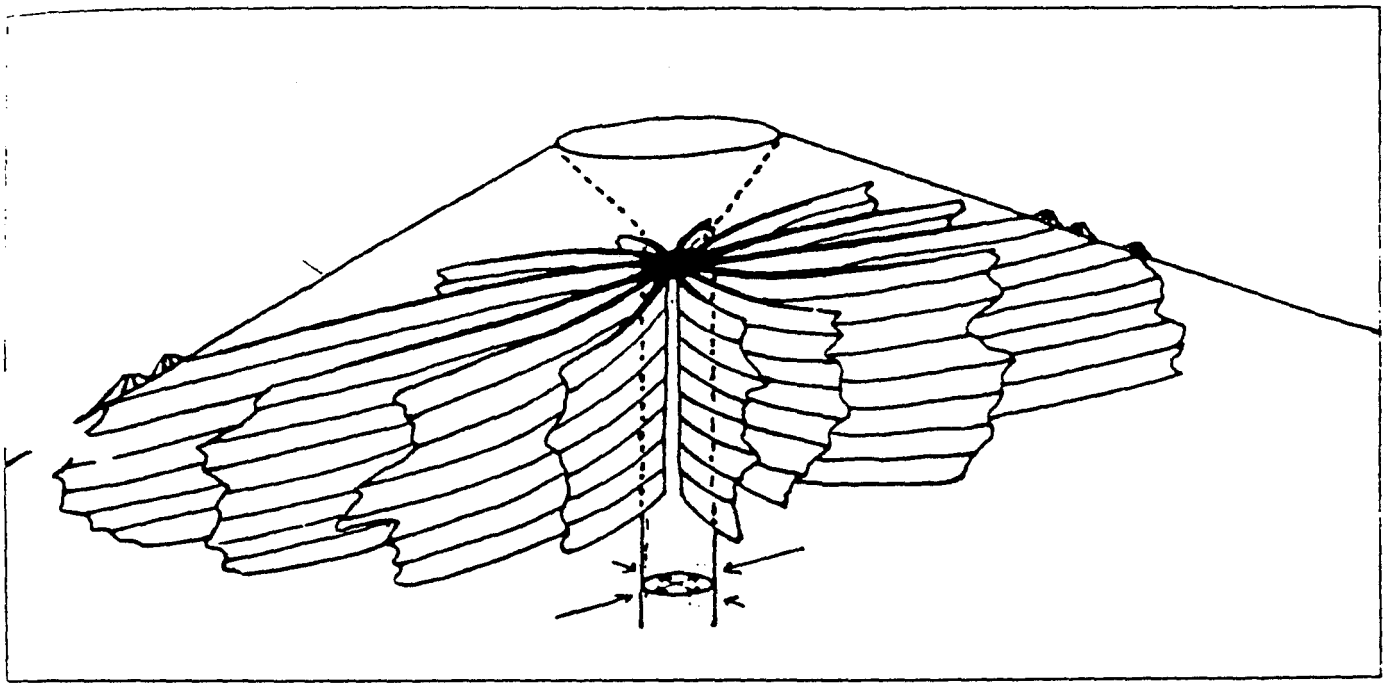

Fig.3. Diagram showing the radial dikes and flank volcanoes of a polygenetic volcano unde a differential horizontal stress. The zone of flank volcanoes corresponds to the trend of radial dike concentration; hence to the trend of maximum compression of the horizontal component of the ambient stress. (After Nakamura, 1976.) (Nakamura, 1977)

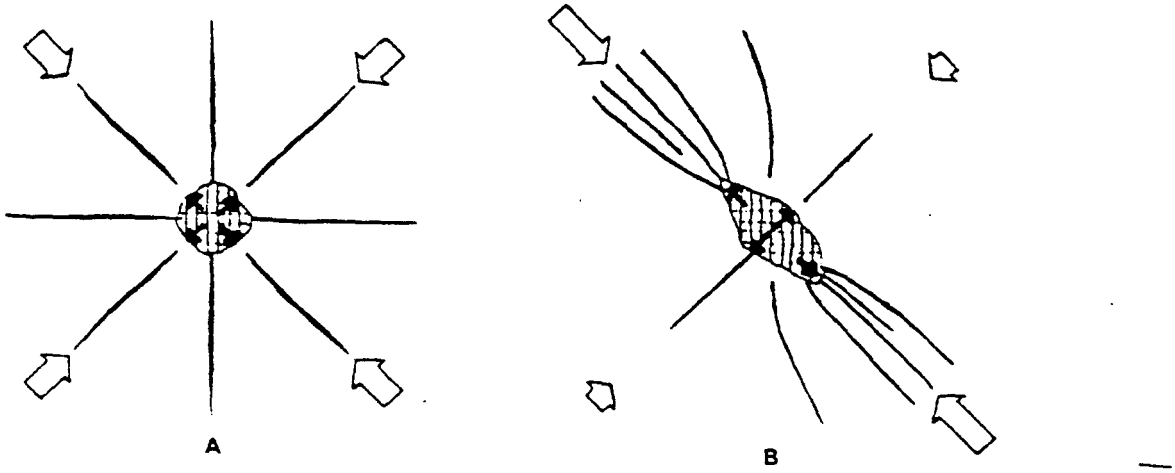

Fig.4 Idealized horizontal cross-section of a conduit of a polygenetic volcano (central plutonic mass) and radial dikes (Nakamura, 1969). A. Perfectly radial dikes under uniform stress. B. Deformed radial dikes under a differential horizontal stress. (Nakamura, 1977)

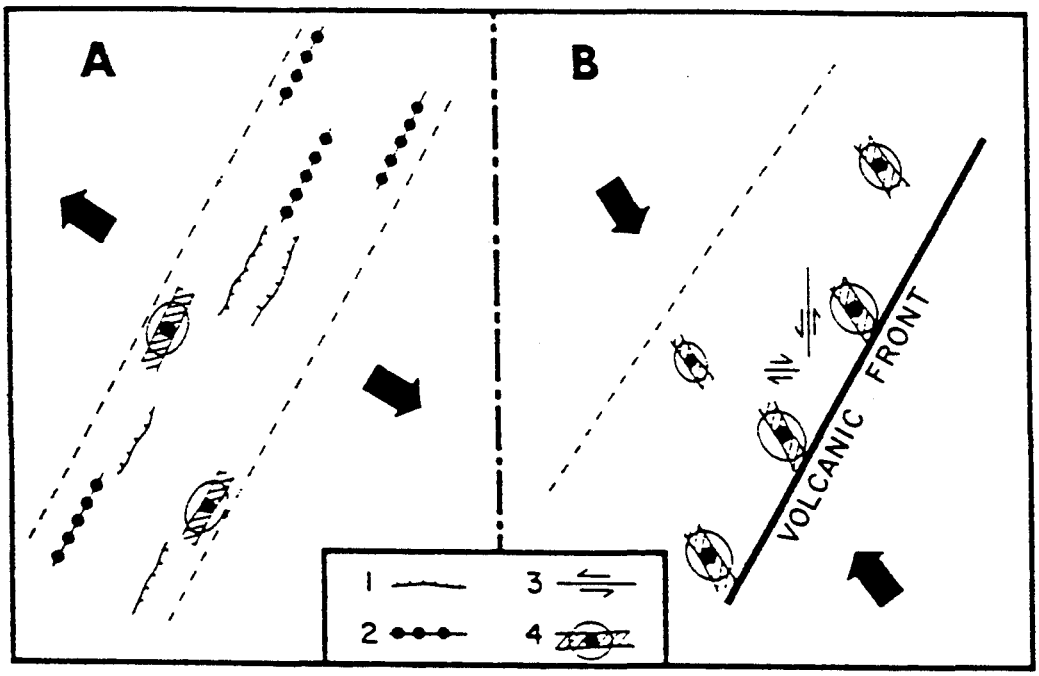

Fig. 5 The angular relationship between the trends of a volcanic belt and zones of flank craters. A and B are idealized situations under extensional and contractional tectonic stres fields. A pair of solid arrows indicates the tensional stress (A) and the compressional stress (B) exerted on the volcanic belt. 1 = a normal fault; 2 = a fissure of regional fissure eruptic 3 = a strike-slip fault; 4 = a polygenetic volcano with a summit crater (dot) and a linear zone of flank eruptions (ruled area). (After Nakamura, 1974.)

(Nakamura, 1977)

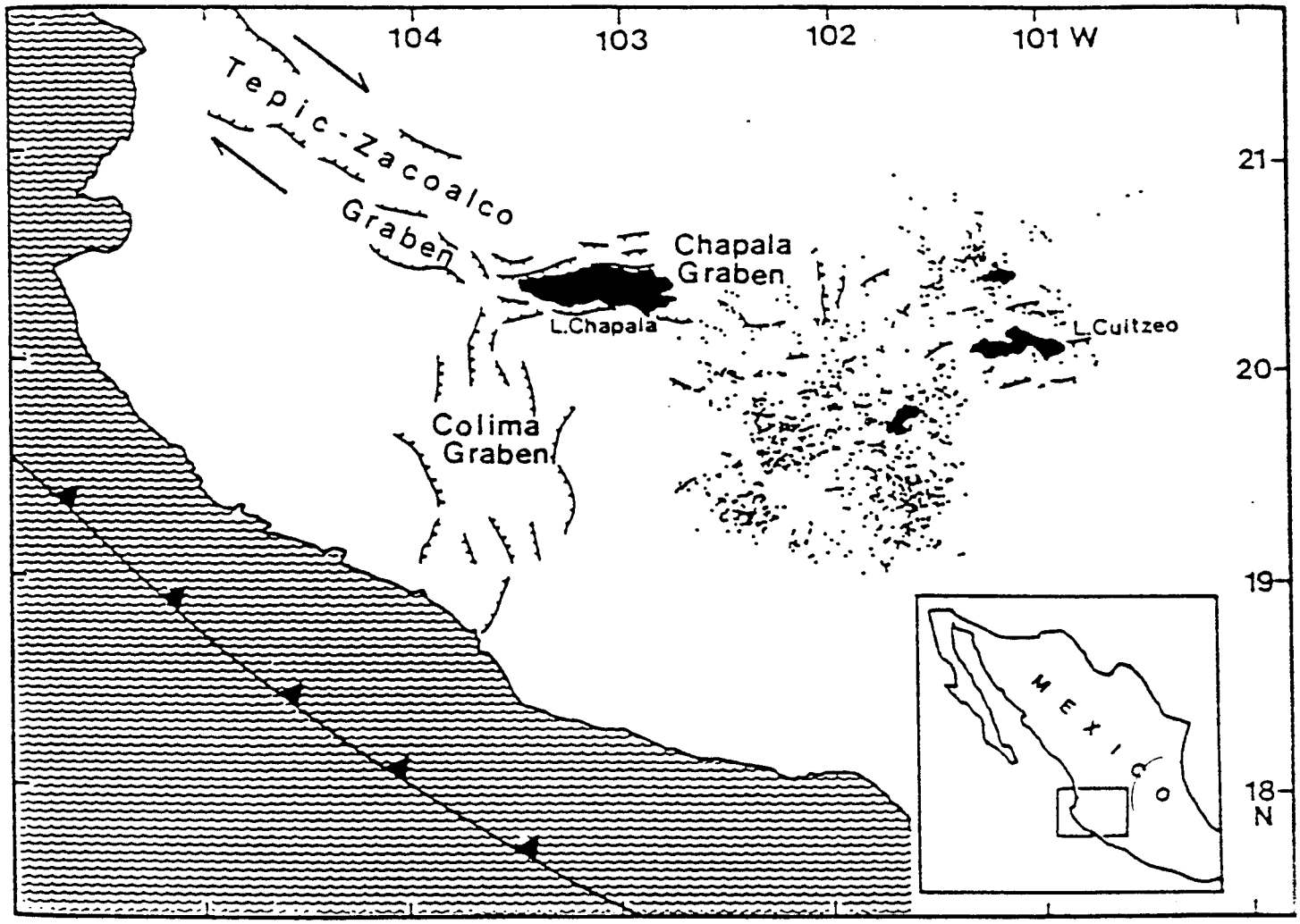

Figure 6 Michoacan-Guanajuato volcanic field (MGVF; black dots) and its regional setting. Trend of subduction zone that gives rise to volcanism is shown in southwest. Principal normal-fault scarps shown are simplified from Allan (1986) and Hasenaka and Carmichael (1985b). Two principal lakes, Chapala (in west) and Cuitzeo (in east), are within weakly defined east-west graben that crosses central part of MGVF. (Wadge and Cross, 1988)

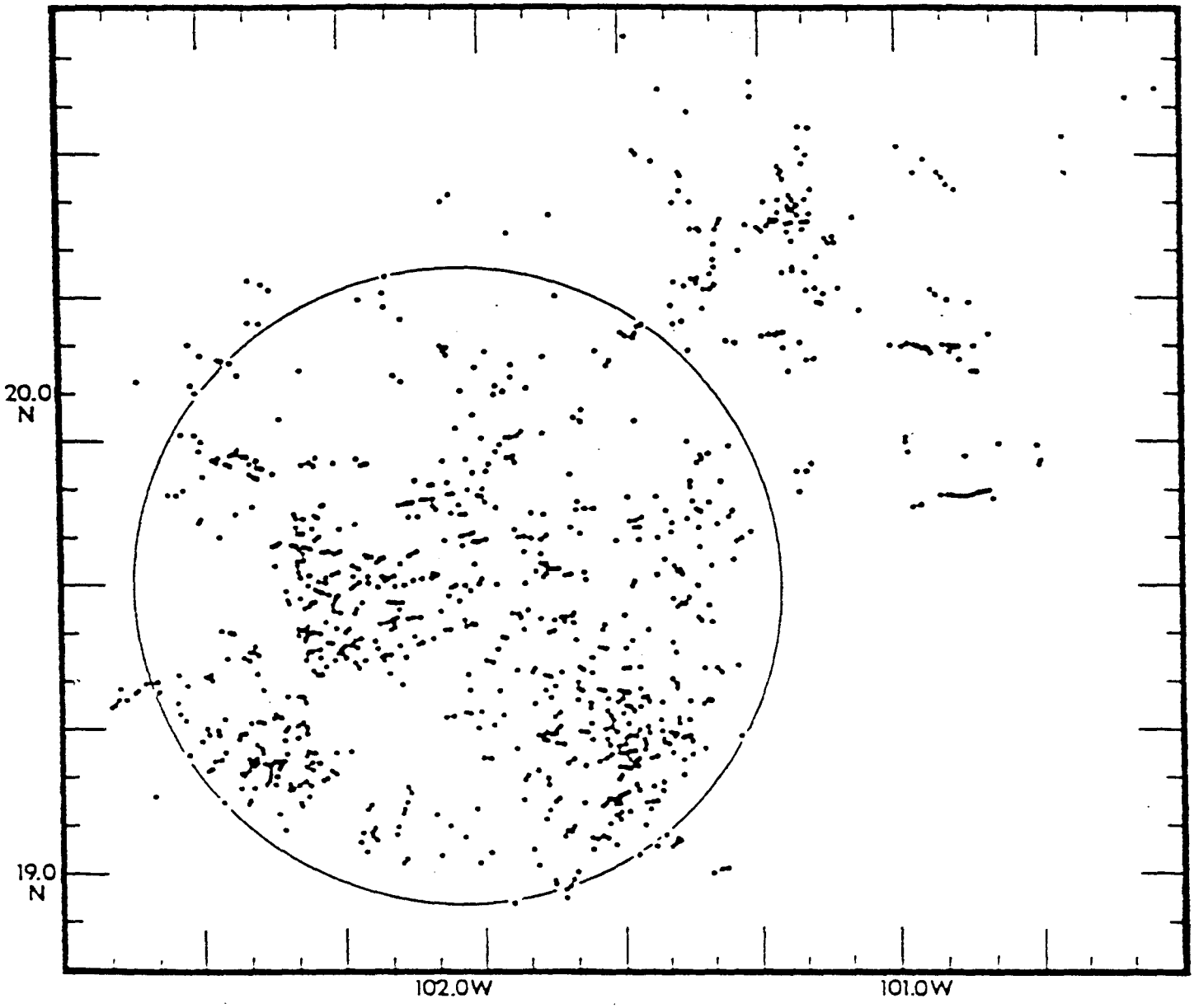

Figure 7 Map of Michoacan-Guanajuato volcanic field as point field of 978 volcanic vent locations. Circle encompasses subset of 778 points. Regional grid used in two-point azimuth method is shown by longer tick marks at margin. (Wadge and Cross, 1988)

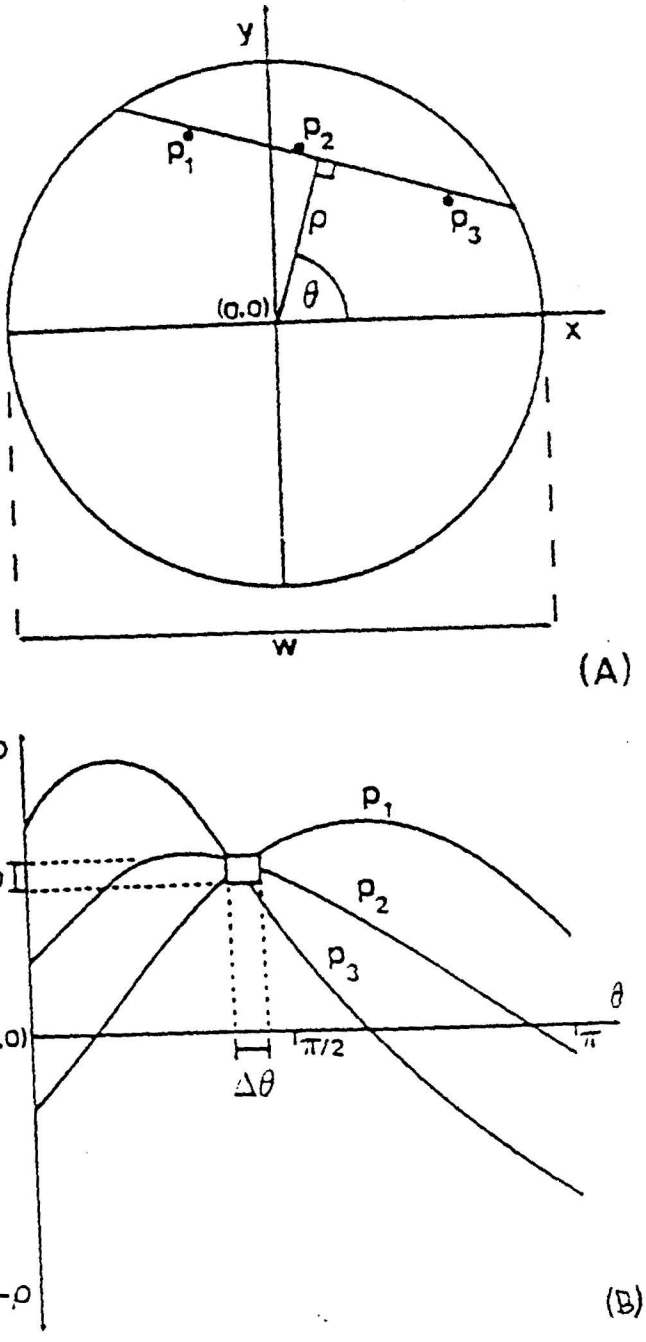

Figure 8 Hough transform method illustration for three nearly collinear points (p). A: x,y plane. B: Corresponding curves in ρ, θ plane

(Wadge and Cross, 1988)

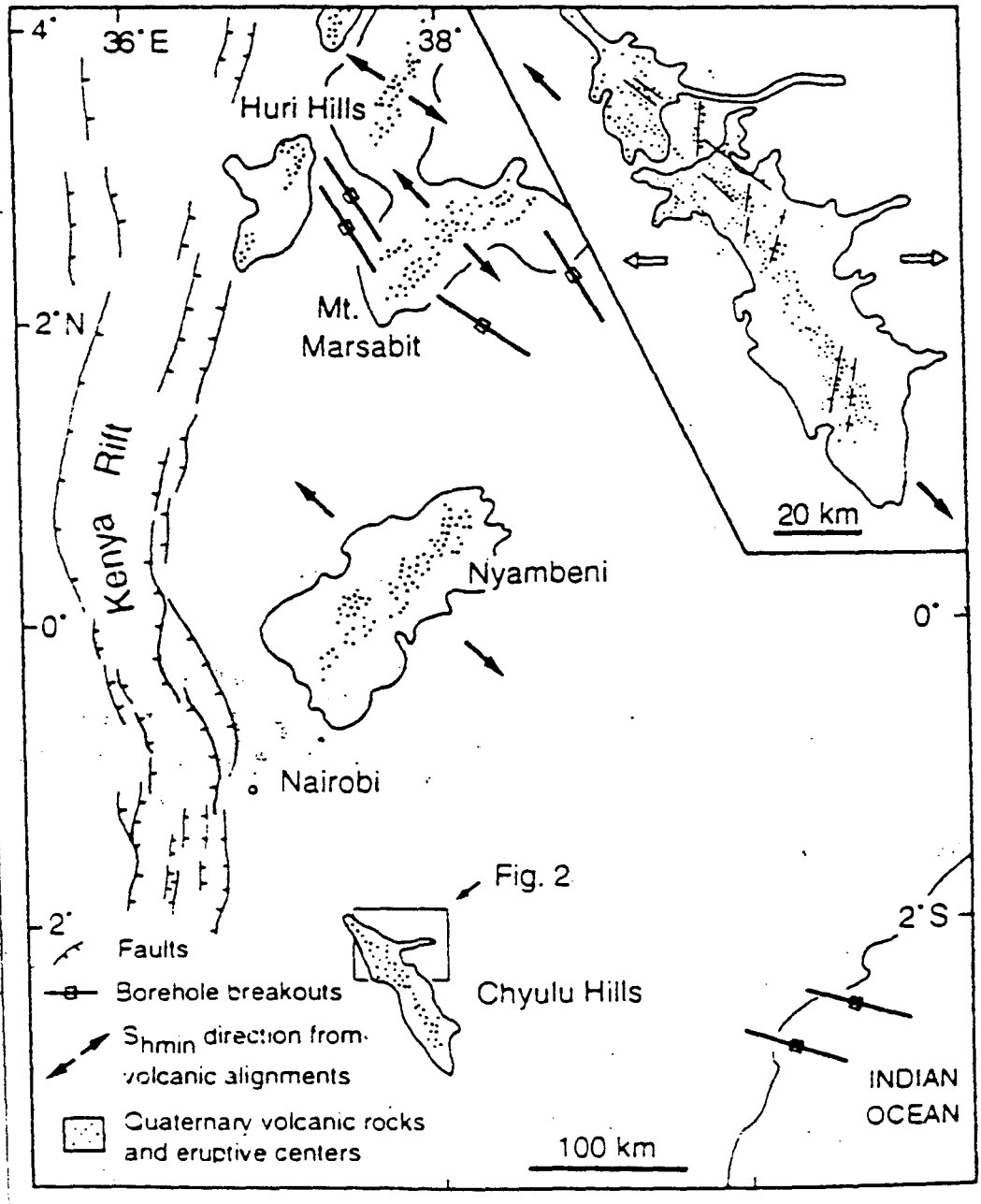

Figure 9. Major faults of Kenya Rift and distribution of Quaternary volcanic rocks and aligned eruptive centers on eastern rift shoulder (redrawn from Saggerson, 1963; Okelo et al., 1988; Strecker and Bosworth, 1991). Inset shows eruptive centers in Chyulu Hills. Open arrows show regional S_{hmin} position prevailing in Kenya until mid-Pleistocene time. Solid arrows show mid-Pleistocene to Holocene S_{hmin} positions. (Haug and Strecker, 1995)

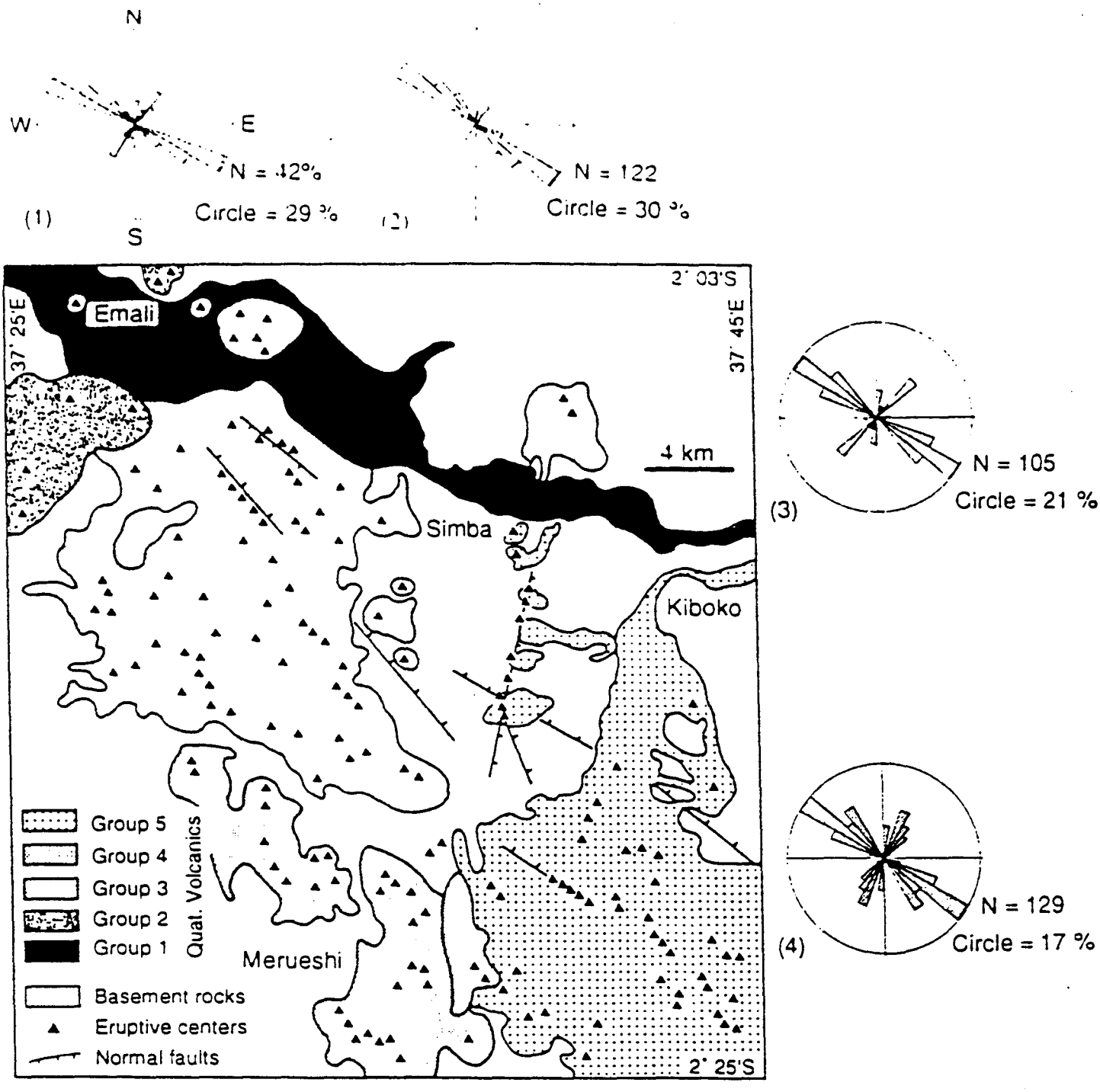

Figure 10. Distribution of aligned eruptive centers, lava-flow units, and normal faults in northern Chyulu Hills. Symmetric rose diagrams display joint distribution in Pan-African basement in area north of Emali (1), north of Simba (2), north of Kiboko (3), and near Merueshi (4).
(Haug and Strecker, 1995)

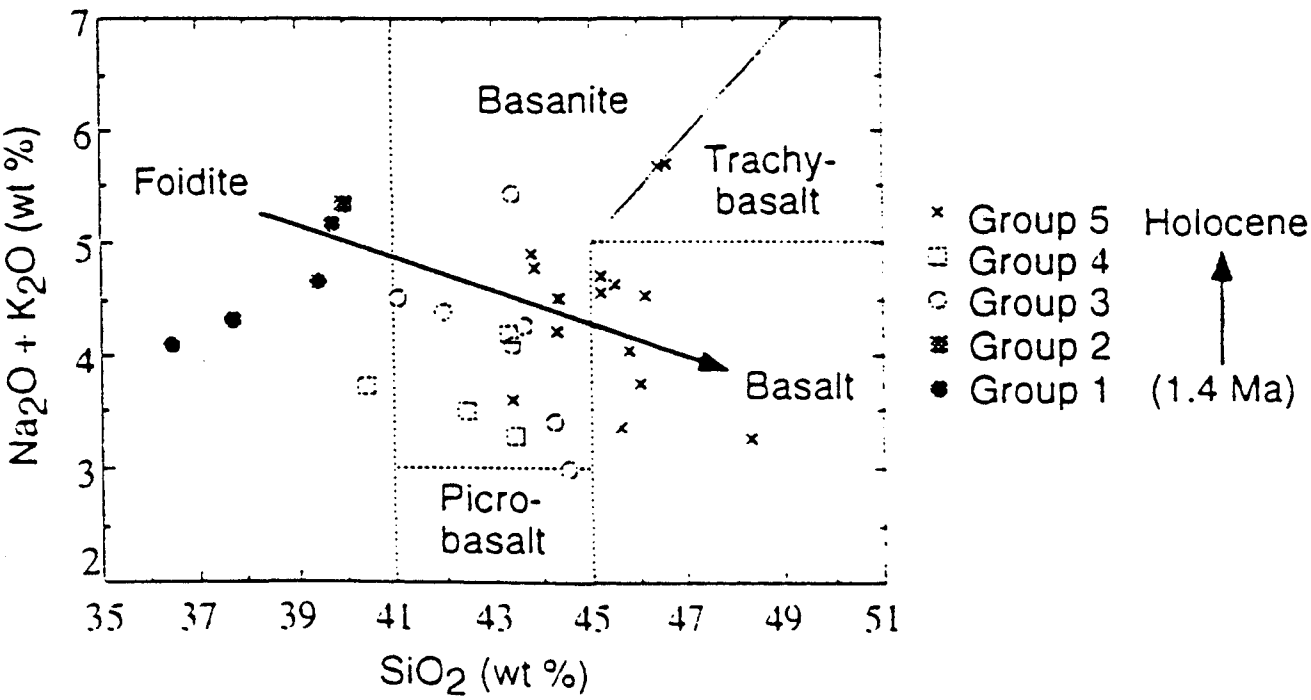

Figure 11 Total alkali and silica classification diagram showing increase in silica content in progressively younger flows in Chyulu Hills. (Haug and Strecker, 1995)

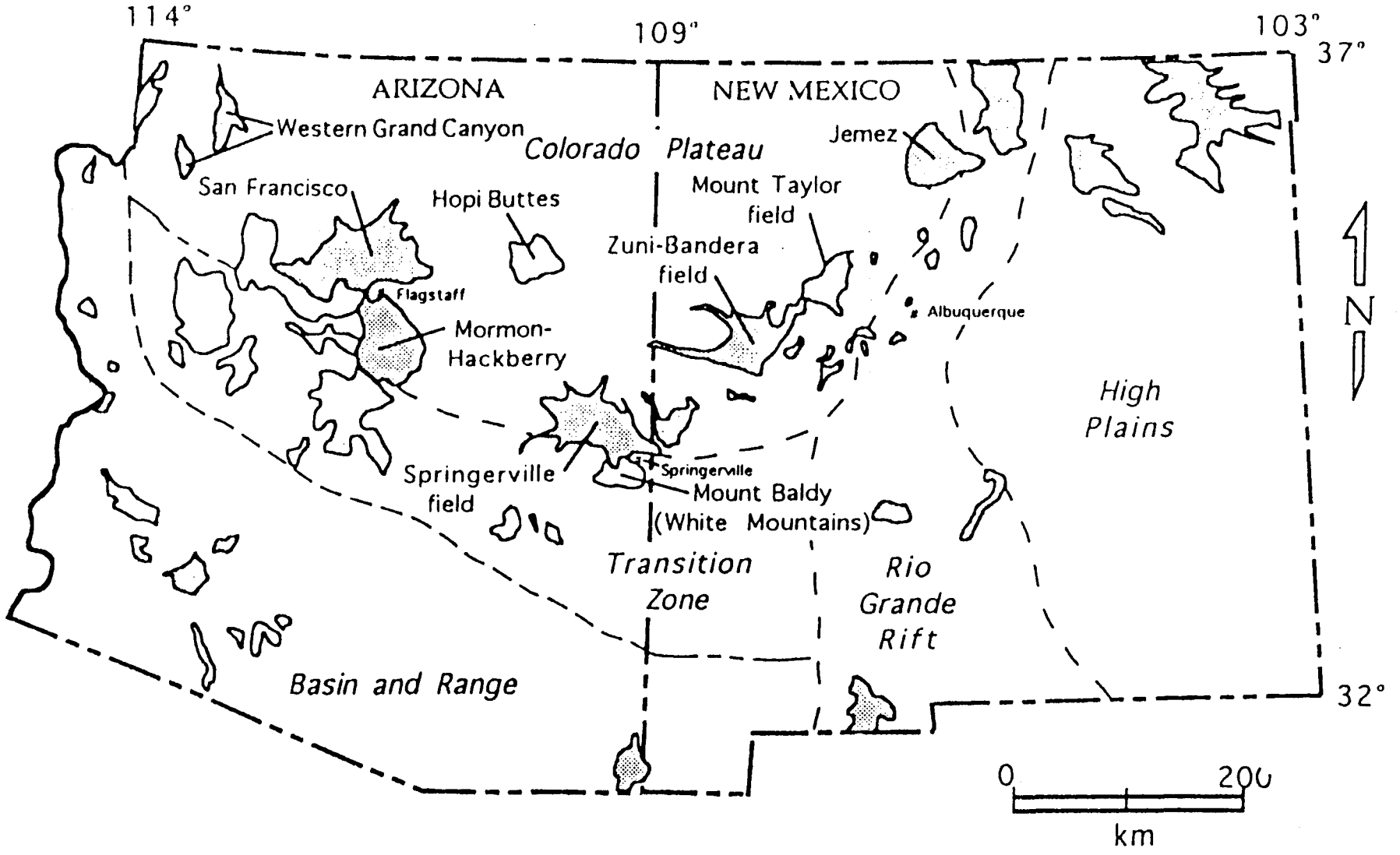

Fig. 12. The Springerville volcanic field is located along the southern margin of the Colorado Plateau, in central east Arizona. Physiographic provinces of the area delineated. The Mogollon Rim is a topographic escarpment which defines the boundary between the Transition Zone and the Colorado Plateau, south of the SVF. Shaded areas indicate volcanic fields less than 5 m.y. old, outlined areas indicate volcanic fields 5 to 16 m.y. old [from *Wolfe et al.*, 1983]. The Jemez lineament [*Aldrich and Laughlin*, 1984] is thought to be comprised of volcanic fields and associated structures extending from the Jemez volcanic field to the southwest, through the Mount Taylor, Zuni-Bandera, and Springerville fields.
(Connor et al., 1992)

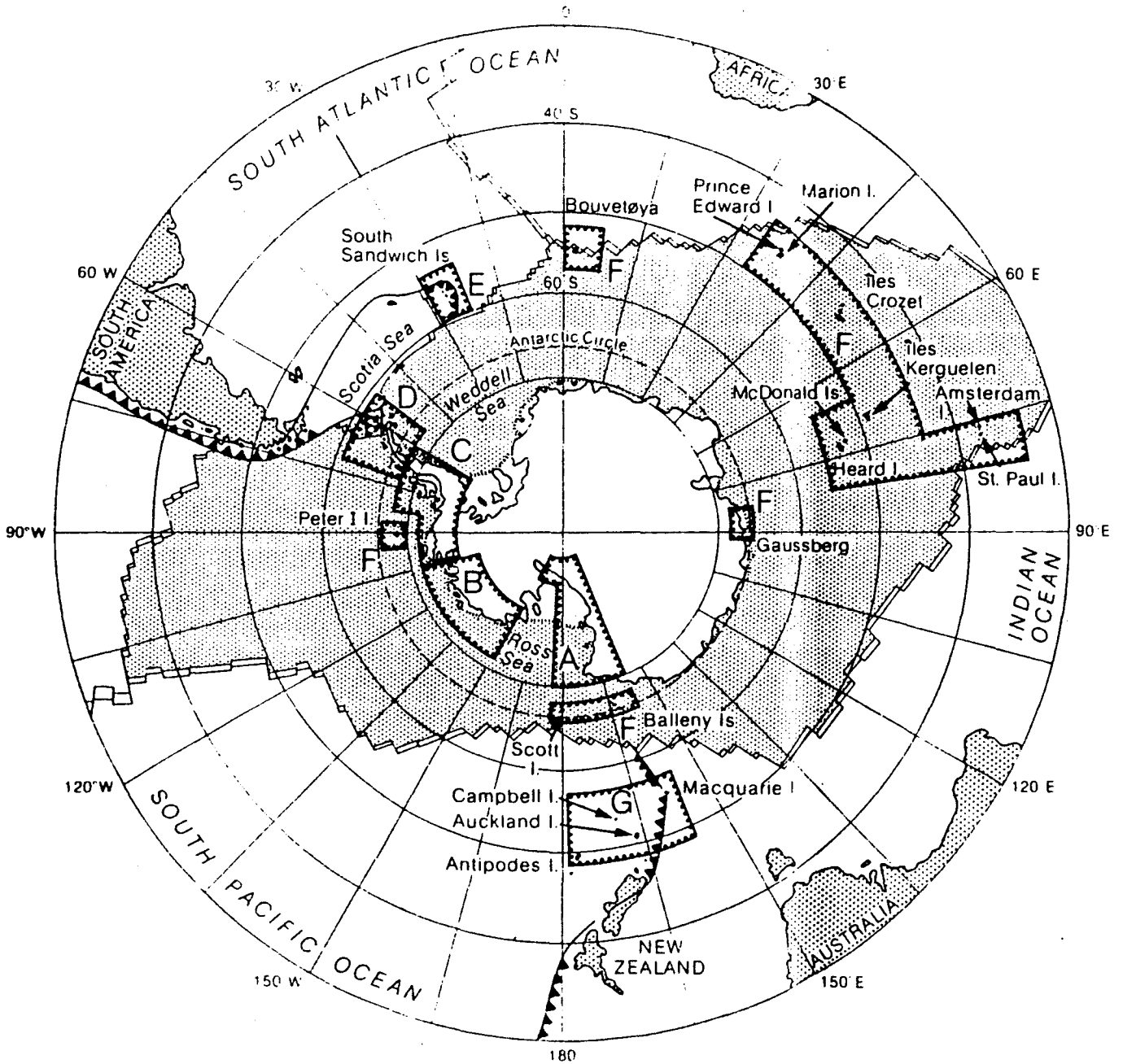

Key

- A McMurdo Volcanic Group - western Ross embayment
- B Marie Byrd Land
- C Alexander Island Palmer Land and Ellsworth Land
- D Graham Land and South Shetland Islands
- E South Sandwich Islands
- F Oceanic islands on the Antarctic plate
- G Subantarctic volcanoes of the Pacific plate

Limits of volcanic regions described in this volume

Antarctic plate oceanic crust

Divergent plate boundary

Transform plate boundary

Convergent plate boundary

Continental areas adjacent to the Antarctic plate

Ice shelves with ice front

0 2000 4000
km

J.W. Thomson 1987

Figure 13
(LeMasurier, 1990)

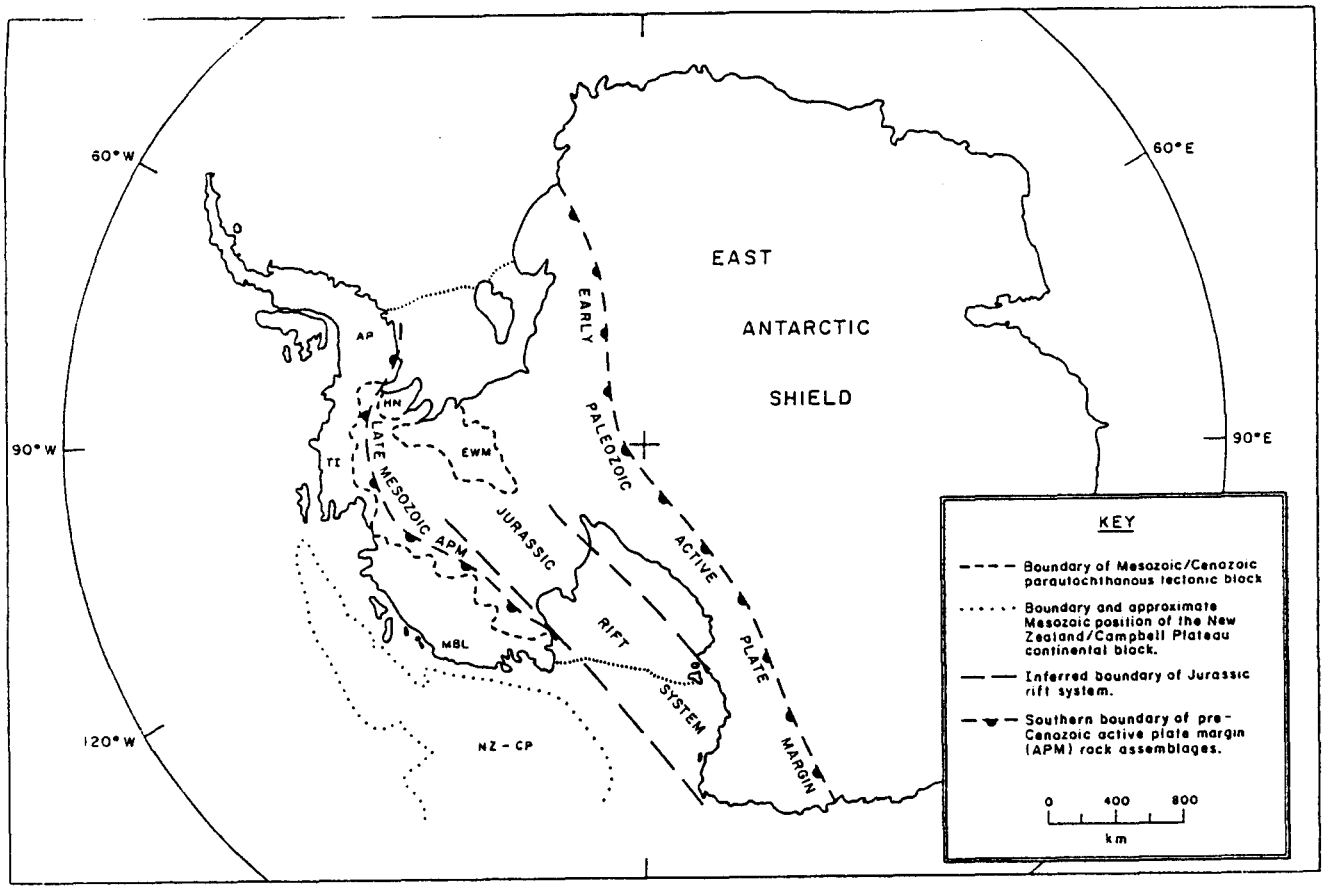

Fig. 14 (opposite) Major tectonic elements of pre-Cenozoic Antarctica. Orogenic belts shown here are the Ross orogen (early Paleozoic) and Andean orogen (late Mesozoic) of *Craddock* [1972], represented here as former active plate margins. The boundary between the two belts is not exposed. Rock assemblages in both belts are dominated by granitoids; the late Mesozoic assemblage is superimposed on middle and late Paleozoic plate margin assemblages, and all three extended into the New Zealand–Campbell Plateau (NZ-CP) block (see *Borg et al.* [1987] for the early Paleozoic and *R.A. Cooper et al.* [1982] for the late Mesozoic). The Jurassic rift system is inferred from the distribution of Jurassic flood basalt, diabase sills and gabbro, from multichannel seismic reflection data in the western Ross Sea, and from Jurassic southern hemisphere continental reconstructions. Boundaries shown here are after *Schmidt and Rowley* [1986]. Tectonic blocks are defined by structural trends, lithologies, and paleomagnetic data; boundaries are determined by topography and aeromagnetic data; Mesozoic and Cenozoic displacements are known for some blocks and inferred for others [*Dalziel and Elliot*, 1982; *Dalziel and Grunow*, 1985; Elliot, personal communication, 1989]. Block names are as follows: MBL, Marie Byrd Land; EWM, Ellsworth-Whitmore Mountains; TI and AP, Thurston Island–Antarctic Peninsula; HN, Haag Nunataks. All boundaries are shown in their present-day positions except the NZ-CP block. (LeMasurier, 1990)

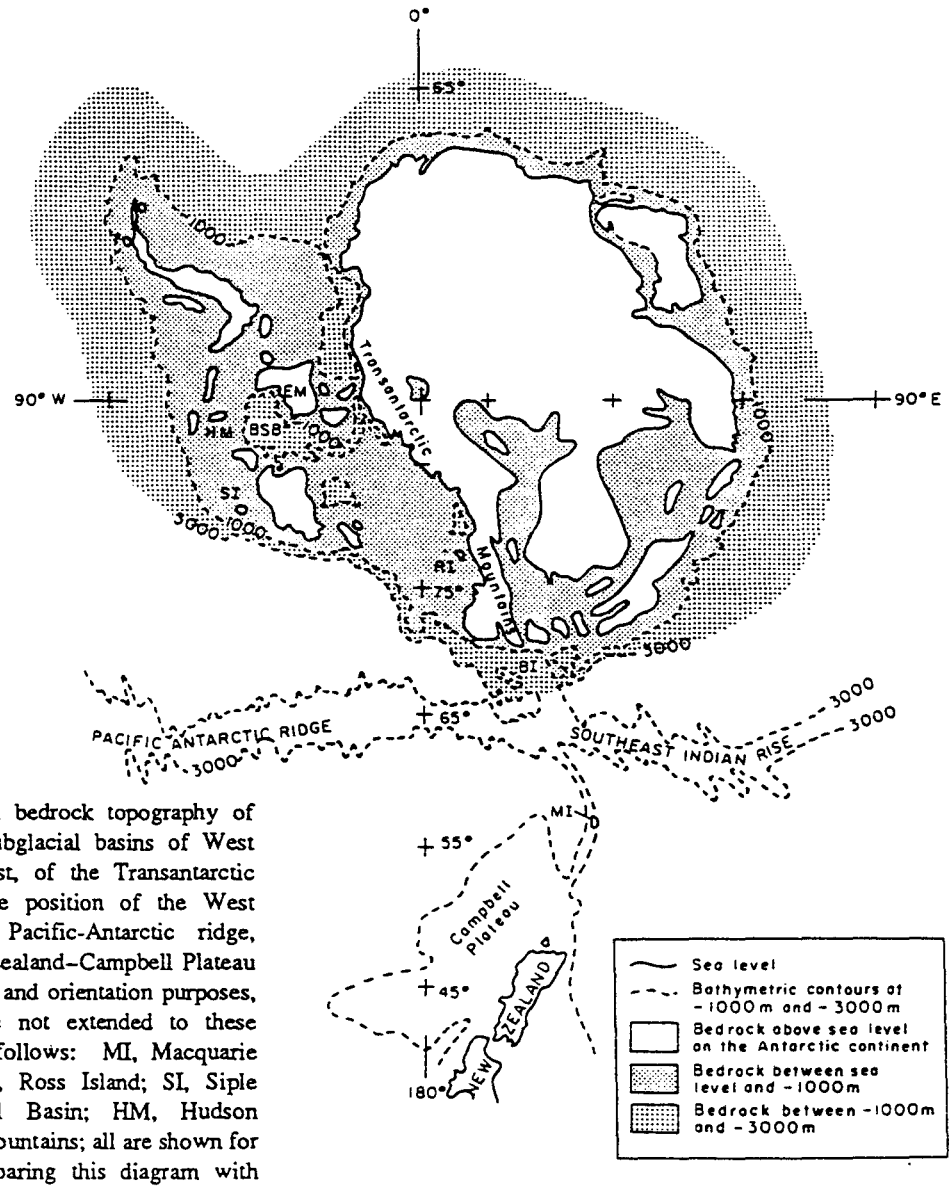

Fig. 15 Generalized subglacial bedrock topography of Antarctica, showing the deep subglacial basins of West Antarctica (the area left, or east, of the Transantarctic Mountains) that help define the position of the West Antarctic rift system. The Pacific-Antarctic ridge, Southeast Indian rise, and New Zealand–Campbell Plateau block are shown for comparative and orientation purposes, but bedrock depth symbols are not extended to these regions. Abbreviations are as follows: MI, Macquarie Island; BI, Balleny Islands; RI, Ross Island; SI, Siple Island; BSB, Byrd Subglacial Basin; HM, Hudson Mountains; and EM, Ellsworth Mountains; all are shown for orientation purposes when comparing this diagram with other diagrams in this volume. Adapted from *American Geographical Society* [1970].

(LeMasurier, 1990)

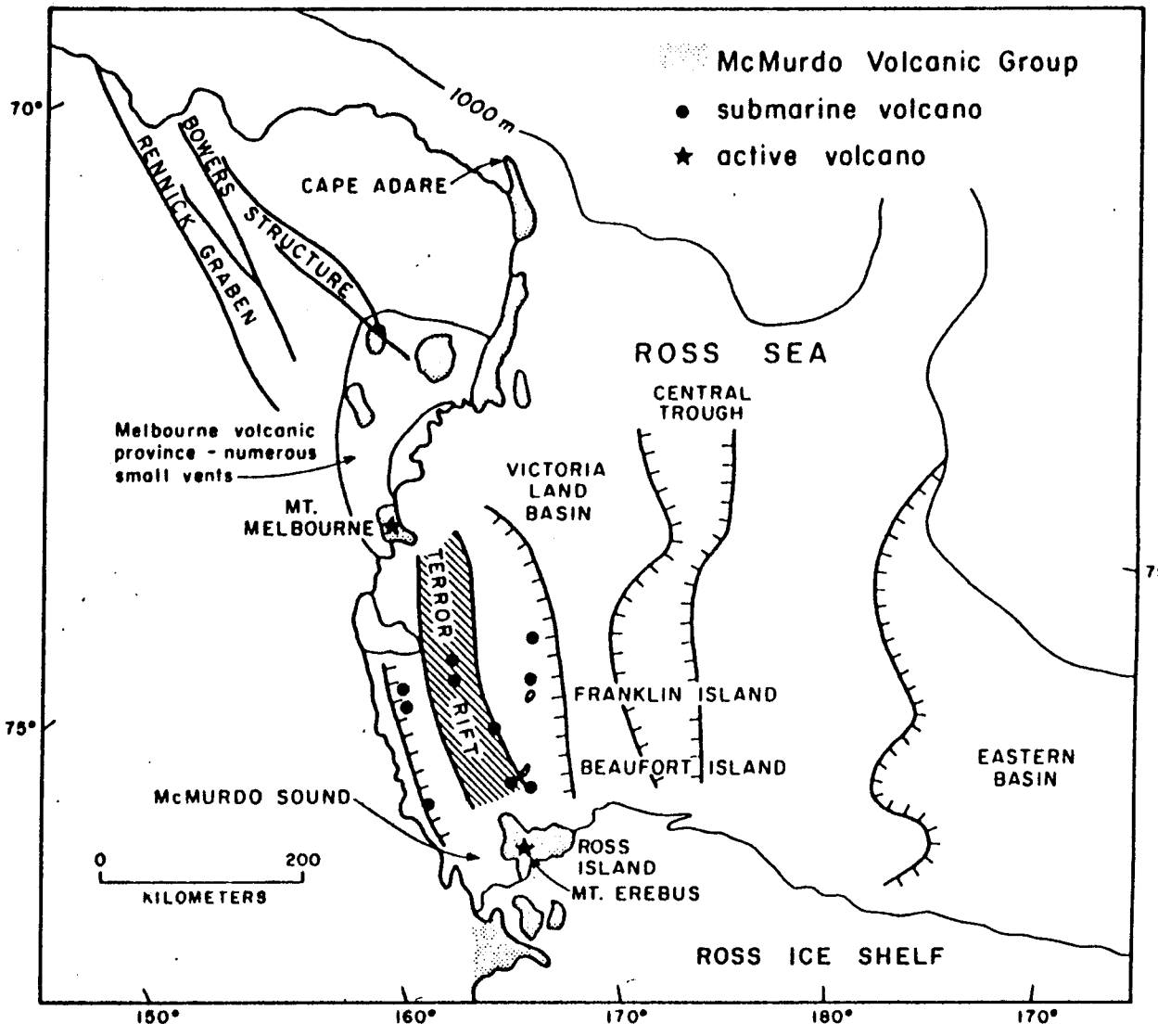

Fig. 16 Simplified tectonic map of the western Ross Embayment, based on work by *Kyle and Cole* [1974], *Cooper et al.* [1987], *Gair et al.* [1969], *Warren* [1969], and *Wright-Grassham* [1987], showing the distribution of McMurdo Volcanic Group rocks along the western margin of the Ross Embayment.

(Kyle, 1990a)

EREBUS VOLCANIC PROVINCE

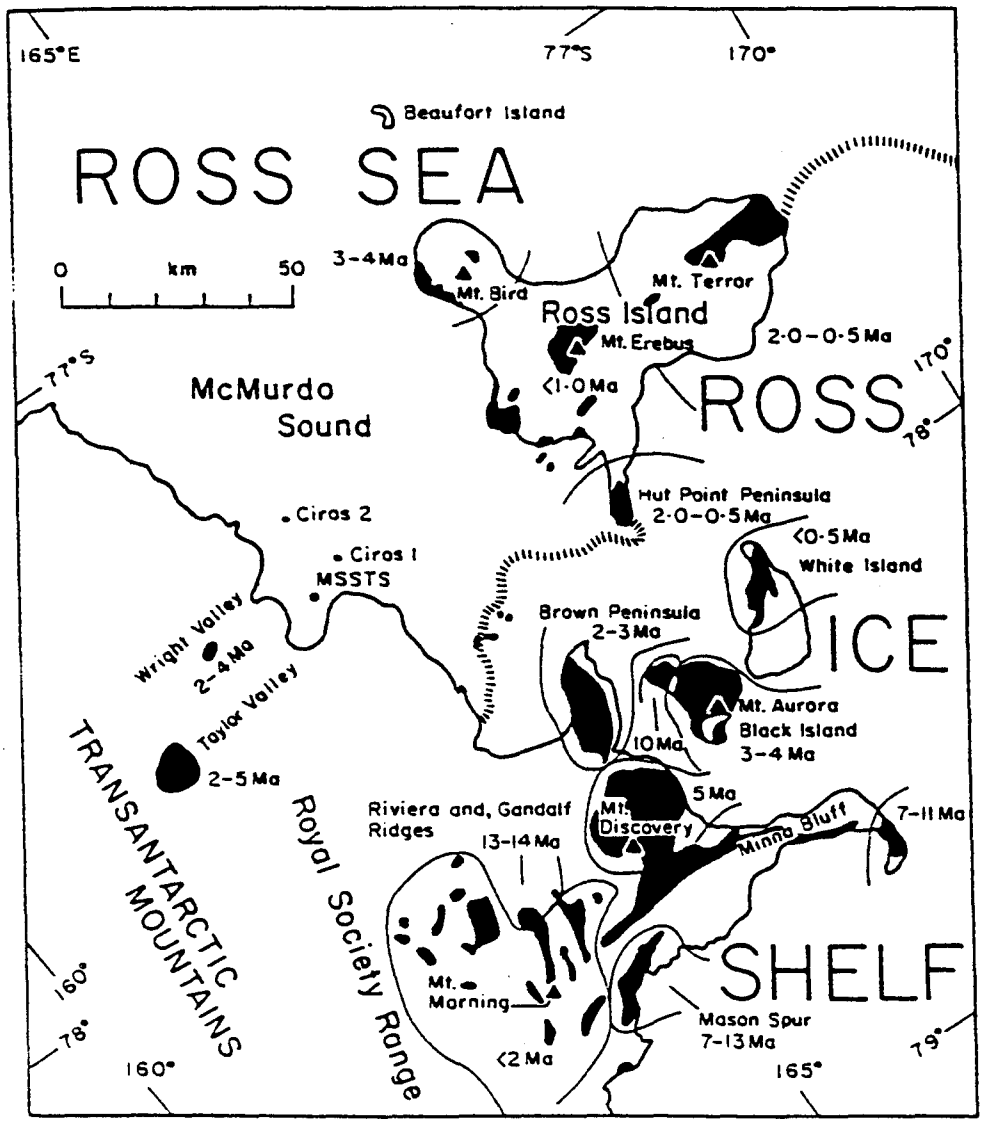

Fig. 17 Generalized ages for the major volcanic centers within the Erebus volcanic province, based mainly on K-Ar age determinations of surficial samples listed in the individual volcano descriptions. (Kyle, 1990b)

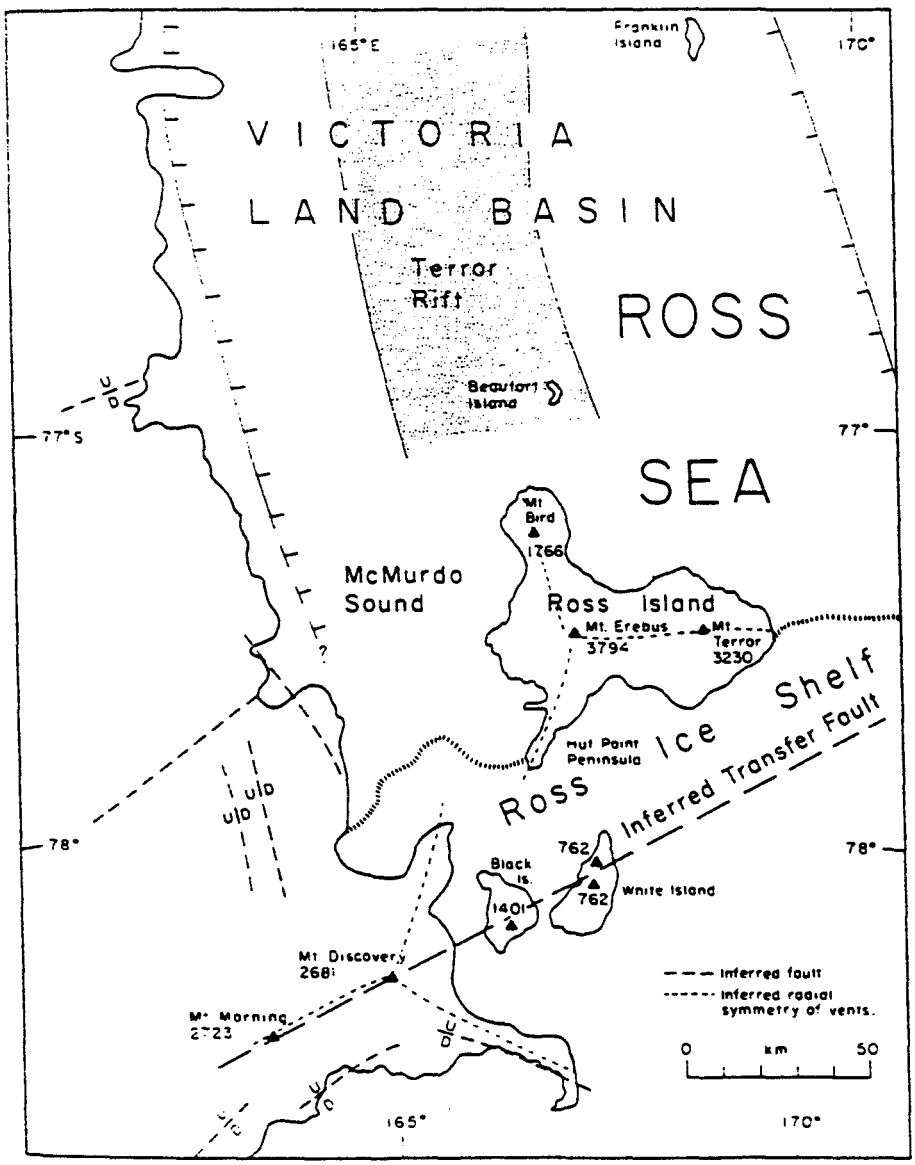

Fig. 18 Generalized tectonic map of Erebus volcanic province, compiled from *Warren* [1969], *Cooper et al.* [1987], *Wright-Grassham* [1987], and Kyle (unpublished observations, 1987).

(Kyle, 1990b)

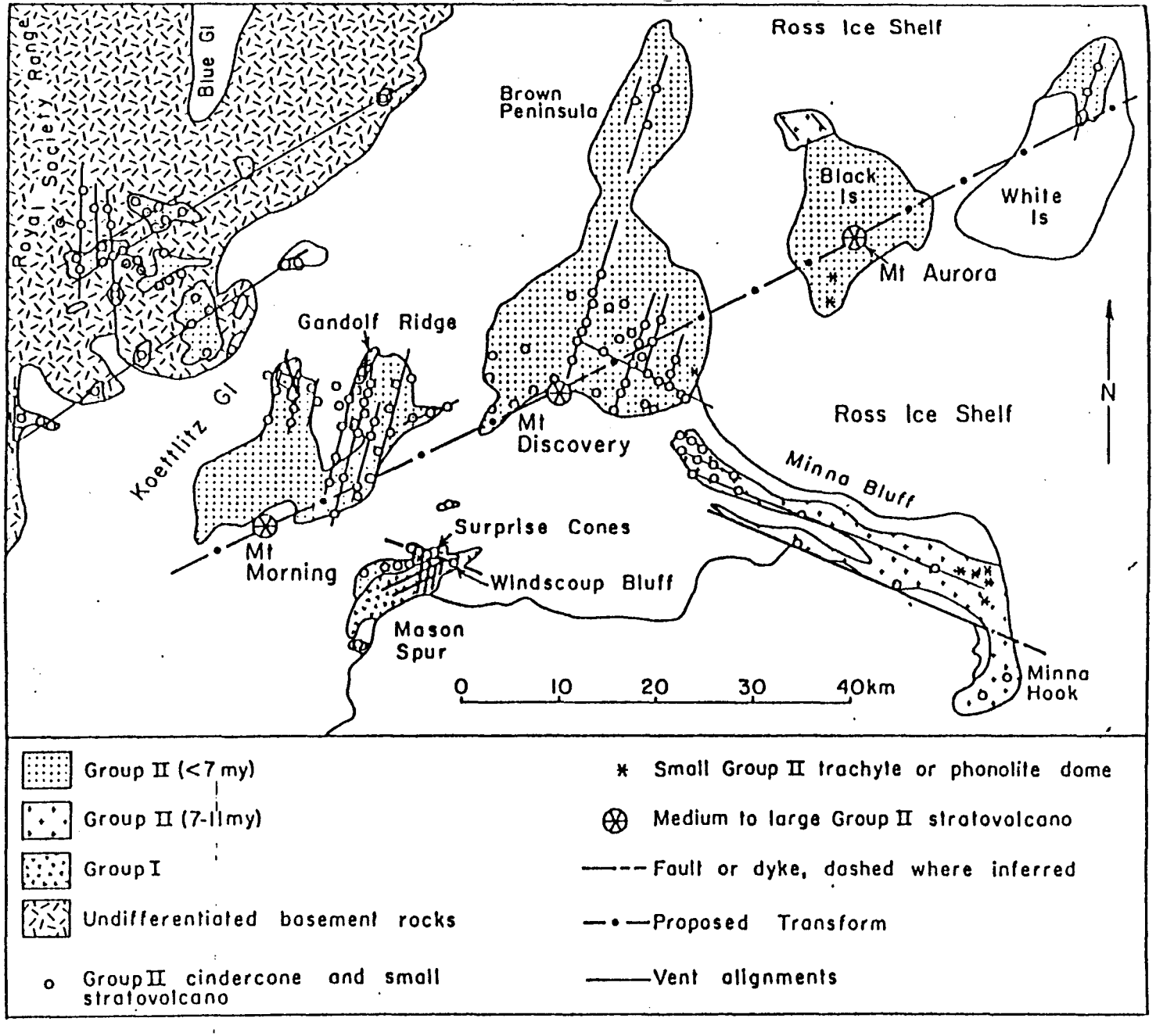

Figure 19 - Structural aspects of the DVS. At Mason Spur, Riviera Ridge, and Gandalf Ridge structural trends are generalized and do not represent specific features. (Wright-Grassham, 1987)